Journal of Alloys and Compounds 511 (2012) 41–44

Contents lists available at SciVerse ScienceDirect

Journal of Alloys and Compounds

journal homepage: www.elsevier.com/locate/jallcom

The suppression and recovery of martensitic transformation in a Ni–Co–Mn–In magnetic shape memory alloy

Z.L. Wang [a], D.Y. Cong [b], Z.H. Nie [a], J. Gao [c], W. Liu [d], Y.D. Wang [a,*]

[a] School of Materials Science and Engineering, Beijing Institute of Technology, Beijing 100081, China
[b] Institute for Metallic Materials, IFW Dresden, P.O. Box 270116, D-01171 Dresden, Germany
[c] Key Laboratory of Electromagnetic Processing of Materials (Ministry of Education), Northeastern University, Shenyang 110004, China
[d] X-Ray Science Division, Argonne National Laboratory, Argonne, IL 60439, USA

ARTICLE INFO

Article history:
Received 3 July 2011
Received in revised form 23 August 2011
Accepted 25 August 2011
Available online 10 September 2011

Keywords:
Undercooling
Martensitic transformation
Non-equilibrium
Magnetic shape memory alloys

ABSTRACT

The intrinsic mechanism of the martensitic transformation (MT) suppression observed in Ni–Co–Mn–In alloys fabricated under non-equilibrium conditions still remains mysterious. Here, we used the undercooling technique to obtain a solidified microstructure in non-equilibrium state, subsequently leading to MT suppression even further cooling to 10 K. It was found that primary dendrite-like In-depleted precipitates occurred during solidification under a large undercooling. After a prolonged annealing, the MT interestingly appeared again due to the dissolution of the precipitates and the recovery of equilibrium chemical composition in the matrix.

1. Introduction

Magnetic shape memory alloys (MSMAs) are regarded as the most promising materials for actuators and dampers based on magnetic-field-induced strain (MFIS) through magnetically induced reorientation (MIR) of martensitic variants [1,2] or magnetically induced phase transformation (MIPT) [3,4]. For the latter mechanism, Ni–Co–Mn–In alloys are particularly attractive since a structural transition from weak magnetic martensite to ferromagnetic austenite can be induced by the application of a magnetic field of several Tesla around room temperature. The interest in the Ni–Co–Mn–In alloys is not only due to their unusual MFIS, but also related to their magnetocaloric effect (MCE) including conventional and inverse cases [5]. Recently a large inverse MCE in $Ni_{45}Co_5Mn_{37.5}In_{12.5}$ single crystal above 300 K was reported, which is promising for magnetic refrigeration applications [6]. However, large hysteresis losses ($H_h > 2$ T) originating from the first-order transition lower the magnetic refrigeration efficiency. Karaca et al. suggested that the hysteresis might be reduced by improving the lattice compatibility between martensite and austenite by introduction of coherent precipitates [7]. The rapid solidification technique based on a large undercooling has been used for fabrication of various functional magnetic materials with homogeneous chemical composition and a grain-refined microstructure [8,9]. It is known that the degree of undercooling ΔT (defined as $\Delta T = T_M - T_N$, where T_M and T_N stand for the melting and nucleation temperatures, respectively) has a significant influence on the microstructure, crystal structure and thermal properties such as transformation temperature for shape memory alloys [10]. Here, the morphology and magnetic and thermal properties of $Ni_{45}Co_5Mn_{36.7}In_{13.3}$ alloys solidified at different undercoolings of 5 K and 69 K followed by respective annealing for 10 h and 72 h were systematically studied. It is shown that large undercooling (i.e. $\Delta T = 69$ K) leads to martensitic transformation suppression due to formation of a novel microstructure showing dendrite-like precipitates in the matrix. After a prolonged annealing, the precipitates vanish and the transformation is observed again. This study establishes the relationships among non-equilibrium solidification with different undercoolings, martensitic transformation and magnetic behaviors, which provides new insights into fundamental phenomena occurring during fabrication of novel magnetic shape memory alloys.

2. Experimental

Ni–Co–Mn–In ingots with nominal composition $Ni_{45}Co_5Mn_{36.7}In_{13.3}$ (at.%) were prepared by arc-melting of pure metals in an argon atmosphere for 5 times. Then lumps of the ingots were placed on borosilicate glass powder and remelted in a high-frequency induction heating apparatus under the protection of argon atmosphere of high purity so as to denucleate the alloy by reaction, adsorption, and passivation of catalytic sites. Each sample was melted, superheated and solidified several

* Corresponding author. Tel.: +86 10 6891 8758.
E-mail addresses: ydwang@mail.neu.edu.cn, ydwang@bit.edu.cn (Y.D. Wang).

0925-8388/$ – see front matter © 2011 Elsevier B.V. All rights reserved.
doi:10.1016/j.jallcom.2011.08.098

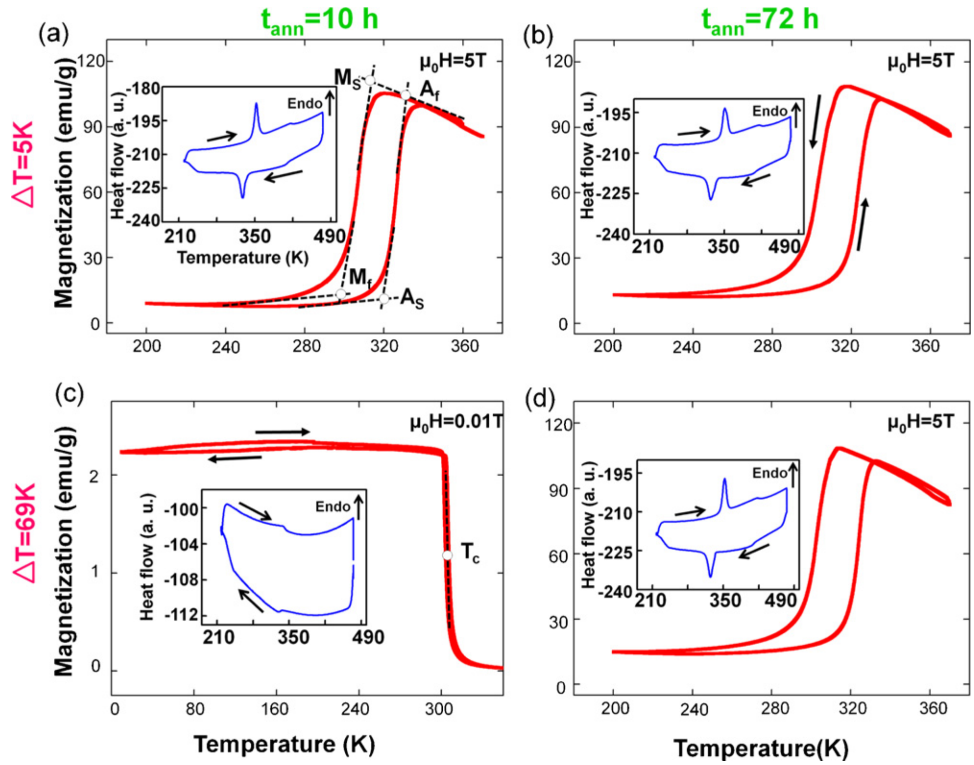

Fig. 1. $M(T)$ curves and DSC curves for $Ni_{45}Co_5Mn_{36.7}In_{13.3}$ alloys. $M(T)$ curves under a constant magnetic field of 5 T in (a), (b) and (d), and 0.01 T in (c) for $Ni_{45}Co_5Mn_{36.7}In_{13.3}$ alloys prepared with different undercoolings and annealed for different time. The insets show the DSC curves (heating and cooling cycles).

times in order to obtain large undercooling. After the high-frequency power source was turned off, the alloy sample was cooled spontaneously. The temperature of the samples was measured by a single-color pyrometer with a relative accuracy and a response time of ±5 K and 10 ms, respectively. Two different undercoolings (ΔT = 5 K, ΔT = 69 K) were attained. Then the two alloys were annealed at 1123 K for 10 h and 72 h. The phase transformation behaviors of the alloys were studied by differential scanning calorimetry (DSC) in the temperature range of 223–486 K, with a heating and cooling rate of 10 K/min. The magnetization versus temperature (i.e., $M(T)$) curves of the alloys were measured using a vibrating sample magnetometer (VSM) in a physical property measurement system (PPMS). The microstructure and morphology of the alloys were examined by optical microscopy and scanning electron microscopy (SEM). The composition distribution and elemental analysis were determined by synchrotron radiation X-ray fluorescence (SRXRF) with a spatial resolution of less than 1 μm. The SRXRF is the emission of characteristic "secondary" (or fluorescent) X-ray from a material that has been excited by bombarding with synchrotron radiation high-energy X-rays.

3. Results and discussion

Fig. 1 shows the $M(T)$ curves of the $Ni_{45}Co_5Mn_{36.7}In_{13.3}$ alloys prepared with undercoolings of 5 K and 69 K, and annealed for different time. DSC curves of these alloys are displayed in the insets of Fig. 1. The alloys with ΔT = 5 K, t_{ann} = 10 h and ΔT = 5 K, t_{ann} = 72 h show obvious martensitic transformation (as an example, the transformation temperatures M_s, M_f, A_s and A_f of the alloy with ΔT = 5 K, t_{ann} = 10 h, under a magnetic field of 5 T, are shown in Fig. 1(a)). However, no martensitic transformation was observed until in the alloy with ΔT = 69 K, t_{ann} = 10 h (see the DSC and $M(T)$ curves in Fig. 1(c)). However, after prolonged annealing, martensitic transformation appears again in the alloy with ΔT = 69 K, t_{ann} = 72 h (see Fig. 1(d)). The different phase transformation behaviors of the alloys prepared with different undercoolings indicate that undercooling has a critical influence on the transformation behavior of the alloys. The other interesting feature is the different magnetic transition behaviors of these alloys, as discussed below. In Fig. 1(c), the abrupt change of the magnetization at ∼330 K corresponds to the Curie transition of austenite at its Curie temperature T_c in the alloy with ΔT = 69 K, t_{ann} = 10 h, which is in general agreement with the Curie transition indicated by the inflection on the DSC curve between 325 K and 350 K (see inset of Fig. 1(c)). It should be noted that the discrepancy between the heating and cooling branches of the $M(T)$ curve in Fig. 1(c) is artificial due to the temperature control of the system. The DSC curves in the insets of Fig. 1 show that T_c of the alloys with ΔT = 5 K, t_{ann} = 10 h and ΔT = 5 K, t_{ann} = 72 h is almost the same (between 400 K and 425 K), but that the T_c of the alloy with ΔT = 69 K, t_{ann} = 10 h is much lower (between 325 K and 350 K). After prolonged annealing, T_c of the alloy with ΔT = 69 K, t_{ann} = 72 h increases and becomes almost the same as that of the alloys with ΔT = 5 K, t_{ann} = 10 h and ΔT = 5 K, t_{ann} = 72 h.

In order to reveal the reason for the anomalous transformation behaviors (i.e. the suppression of the martensitic transformation and the lowering of the Curie temperature) in the alloy with ΔT = 69 K, t_{ann} = 10 h, microscopic study of the alloys was conducted. It was found that at room temperature the alloys with ΔT = 5 K, t_{ann} = 10 h and ΔT = 5 K, t_{ann} = 72 h has a typical stripe-like martensitic microstructure (Fig. 2(a) and (b)). In contrast, the alloy with ΔT = 69 K, t_{ann} = 10 h exhibits a novel morphology consisting of dendrite-like precipitates dispersed in the matrix (Fig. 2(c)). A similar morphology was also observed in the as-cast alloy. Therefore, it can be concluded that the novel morphology forms during non-equilibrium solidification rather than during annealing. However, after prolonged annealing, the precipitates disappear and a stripe-like martensitic microstructure appears again in the alloy with ΔT = 69 K, t_{ann} = 72 h (Fig. 2(d)). This indicates that during the prolonged annealing the precipitates forming under non-equilibrium solidification conditions are dissolved into the matrix at elevated temperature, resulting in a homogenous single phase that transforms into martensite at lowered temperature during cooling, which are preserved down to room temperature. During non-equilibrium solidification at the larger undercooling of

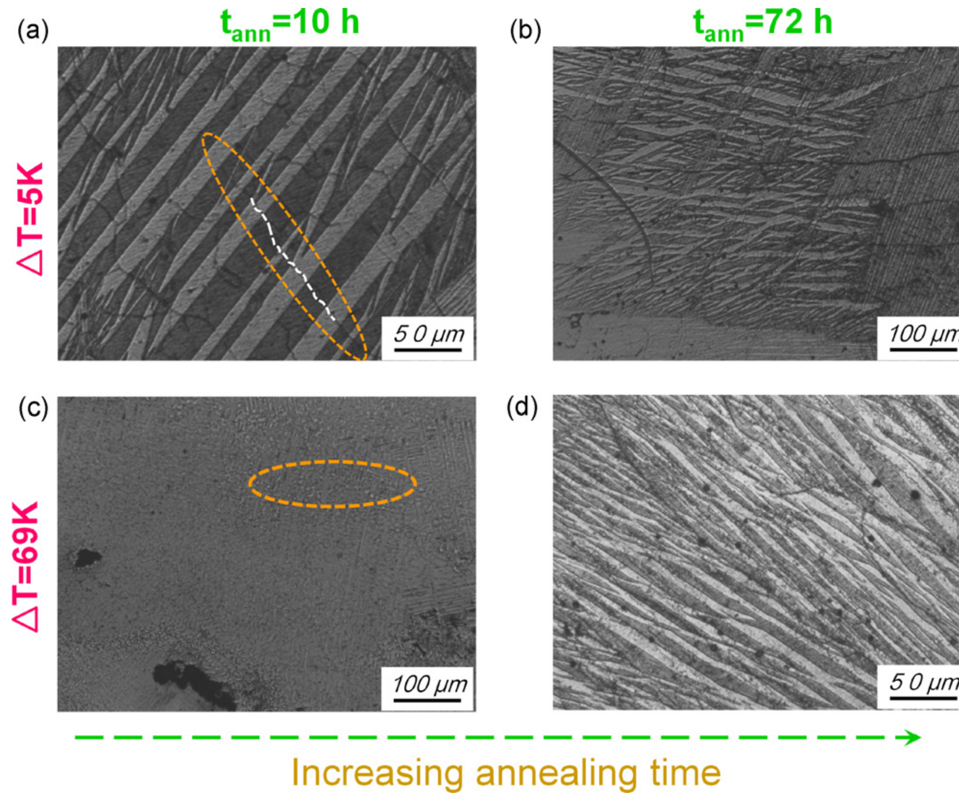

Fig. 2. Microstructure of the alloys prepared with an undercooling of 5 K and annealed for 10 h (a) and 72 h (b) and with an undercooling of 69 K and annealed for 10 h (c) and 72 h (d), respectively. The grain boundary is depicted by the white dashed line [within the zone surrounded by orange dashed line in (a)]. The precipitates dispersed in the matrix (dashed ellipse) are illustrated in (c). (For interpretation of the references to color in this figure legend, the reader is referred to the web version of the article.)

69 K, the dendrite-like precipitates form as primary phase followed by the formation of austenite. Subsequently, the chemical composition of austenite is greatly altered off the equilibrium state. The SEM backscattered electron image on the morphology of the dendrite-like precipitates in the matrix is shown in Fig. 3(a). The composition mapping of Ni, Mn, Co, and In elements by SRXRF is shown in Fig. 3(b). The intensity of characteristic fluorescent X-rays is proportional to the concentration of the elements. The SRXRF

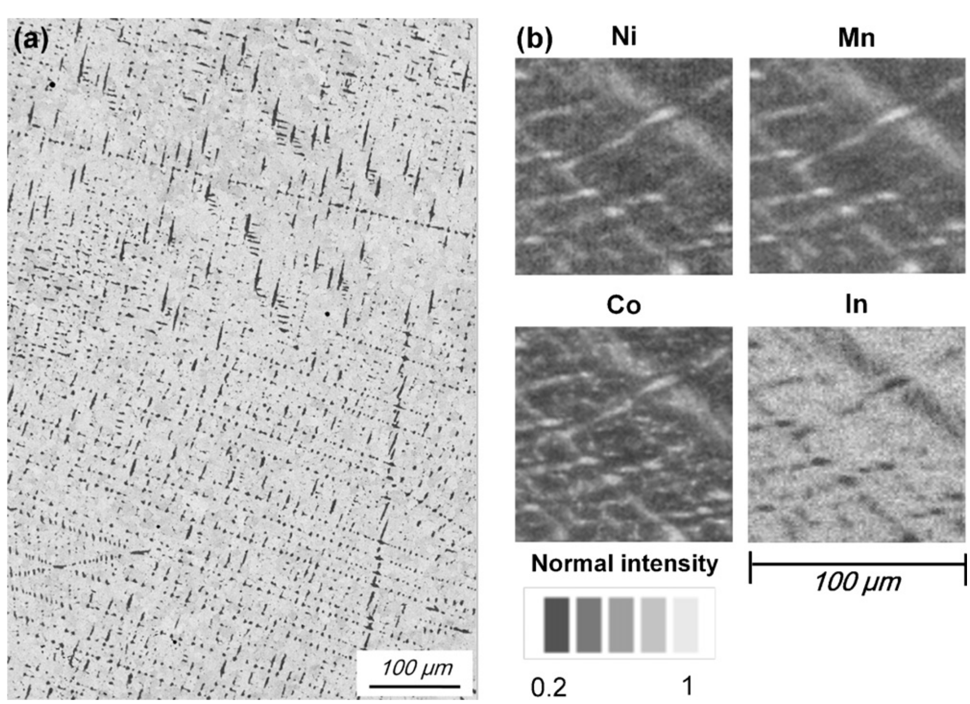

Fig. 3. SEM backscattered electron image of the alloy prepared with an undercooling of 69 K and annealed for 10 h in (a) as well as distributions of the Ni, Mn, Co and In elements determined by SRXRF (b).

maps provide the accurate information on the distribution of the elements so that the contours of different phases can be readily recognized. Here, the maps show clearly that the precipitates in the alloy with $\Delta T = 69$ K, $t_{ann} = 10$ h are dendrite-like and depleted in Indium compared to the matrix around. Thus, the matrix is rich in Indium, which leads to the decrease in the value of *e*/*a*. According to the *e*/*a* dependence of Ms temperature found in Ni–Mn–In alloys [11], the decrease in *e*/*a* finally should result in the suppression of martensitic transformation in the Co-doped Ni–Mn–In alloy. The annealing at high temperature for sufficient time leads to recovery of the equilibrium state again. That explains why martensitic transformation is suppressed in the alloy with $\Delta T = 69$ K, $t_{ann} = 10$ h but it appears again in the alloy with $\Delta T = 69$ K, $t_{ann} = 72$ h. Furthermore, it is reasonable to suppose that the non-equilibrium solidification and the final microstructure also account for the temperature decrease in T_c in the alloy with $\Delta T = 69$ K, $t_{ann} = 10$ h compared to that in other alloys.

The preliminary indexing of electron backscatter diffraction (EBSD) suggests that the precipitates are tetragonal structure, whereas the matrix is cubic with a Heusler-type structure. The details of the crystal structure such as accurate lattice parameters are still worth of further study. Interestingly, martensite variants seem to crossover the grain boundaries as highlighted with ellipse circle in Fig. 2(a). Generally, this phenomenon is usually found in the samples consisting mainly of low-angle grain boundaries [12].

4. Conclusion

To summarize, the suppression and recovery of martensitic transformation in the $Ni_{45}Co_5Mn_{36.7}In_{13.3}$ alloy with a large undercooling ($\Delta T = 69$ K) was studied. The non-equilibrium solidification prepared with a large undercooling ($\Delta T = 69$ K) leads to the formation of a novel microstructure consisting of primary dendrite-like precipitates, which are depleted in In-element in the matrix of a Heusler phase. Consequently, martensitic transformation is suppressed, and the Curie temperature is lowered. Prolonged annealing induces dissolution of the precipitates, allowing the microstructure to recover its equilibrium state and martensitic transformation to resume.

Acknowledgements

This work is supported by the National Natural Science Foundation of China (Grant Nos. 50725102 and 50971031) and National Basic Research Program of China (973 Program) under Contract No. 2012CB619405. Use of the Advanced Photon Source was supported by the U.S. Department of Energy, Office of Science, Office of Basic Energy Science, under Contract No. DE-AC02-06CH11357.

References

[1] K. Ullakko, J.K. Huang, C. Kanter, V.V. Kokorin, R.C. O'Handley, Appl. Phys. Lett. 69 (1996) 1966–1968.
[2] A. Sozinov, A.A. Likhachev, N. Lanska, K. Ullakko, Appl. Phys. Lett. 80 (2002) 1746–1748.
[3] R. Kainuma, Y. Imano, W. Ito, Y. Sutou, H. Morito, S. Okamoto, O. Kitakami, K. Oikawa, A. Fujita, T. Kano-mata, K. Ishida, Nature 439 (2006) 957–960.
[4] Y.D. Wang, E.W. Huang, Y. Ren, Z.H. Nie, G. Wang, Y.D. Liu, J.N. Deng, H. Choo, P.K. Liaw, D.E. Brown, L. Zuo, Acta Mater. 56 (2008) 913–923.
[5] A. Planes, L. Mañosa, M. Acet, J. Phys. Condens. Matter 21 (2009) 233201.
[6] D. Bourgault, J. Tillier, P. Courtois, D. Maillard, X. Chaud, Appl. Phys. Lett. 96 (2010) 132501.
[7] H.E. Karaca, I. Karaman, A. Brewer, B. Basaran, Y.I. Chumlyakov, H.J. Maier, Scripta Mater. 58 (2008) 815–818.
[8] N. Liu, F. Liu, C.L. Yang, Y.Z. Chen, G.C. Yang, Y.H. Zhou, J. Alloys Compd. 465 (2008) 391–395.
[9] N. Liu, F. Liu, G.C. Yang, Y.Z. Chen, D. Chen, C.L. Yang, Y.H. Zhou, Phys. B: Condens. Matter 387 (2007) 151–155.
[10] H.X. Zheng, M.X. Xia, J. Liu, J.G. Li, J. Alloys Compd. 388 (2005) 172–176.
[11] T. Krenke, M. Acet, E.F. Wassermann, X. Moya, L. Mañosa, A. Planes, Phys. Rev. B 73 (2006) 174413.
[12] J. Liu, T.G. Woodcock, N. Scheerbaum, O. Gutfleisch, Acta Mater. 57 (2009) 4911–4920.